

\* This report summarises the outcomes from the UK NC3R's and POEM's Maths Study Group meeting, 8th –12th September 2014 in response to a problem entitled 'Improving the utility of *Drosophila melanogaster* for neurodegenerative disease research by modelling courtship behaviour patterns', presented by BB and CS.

## Improving the utility of *Drosophila melanogaster* for neurodegenerative disease research by modelling courtship behaviour patterns

Birgit Brüggemeier<sup>1</sup>, Christian Schusterreiter<sup>1</sup>, Hania Pavlou<sup>1</sup>, Neil Jenkins<sup>2</sup>, Stephen Lynch<sup>3</sup>, Arianna Bianchi<sup>4</sup>, and Xiaohao Cai<sup>5</sup>

<sup>1</sup>University of Oxford

<sup>2</sup>University of Warwick

<sup>3</sup>Manchester Metropolitan University

<sup>4</sup>Heriot-Watt University, Edinburgh

<sup>5</sup>University of Cambridge

November 28, 2014

## Abstract

Courtship in *Drosophila* is used already to screen genes linked to memory-deficiency and neurodegeneration in humans [14]. We have developed three models of fly courtship to study potential mechanisms underlying this complex behaviour. We have found that dynamics of fly courtship behaviour can be modelled reasonably well as a markovian stochastic process. A stochastic model may help to account for males' interaction with females [6]: the male reacts to female cues and his behaviour is partially driven by them [7]. The female might influence courtship choices in the male by sexually motivating him, as Margaret Bastock suggested in her model of male courtship [9]. In Bastock's theory, sexual motivation determines courtship choices: when sexual motivation exceeds a threshold, the male courts. Each courtship behaviour requires a different level of sexual motivation. We apply Bastock's theory in two neuronal models. We modelled sexual motivation as firing frequency of model neurons. Our preliminary results suggest that our neuronal models can also simulate courtship dynamics. In future research we aim to test whether altered courtship dynamics are picked up by varying the state space of the stochastic model and testing whether a richer set of behaviours will still be fitted as well by such a simple model. We believe stochastic male courtship to indicate functional processing of female cues. In our neuron model approach, we model impaired processing of sexual cues in the male by reduced firing rates of neurons. When firing rates are sufficiently high the whole behavioural space is traversed. We will test how the path through the behavioural space changes when we assume low firing rates. We expect that the path becomes highly cyclical – only behaviours with low excitatory thresholds are shown repeatedly. We are the first to test markovian properties of courtship dynamics and to implement Bastock's ethological model of courtship to mathematical models. We believe that finding the appropriate model parameters for the modeling of fly courtship, might give valuable information on the state of the male fly: is the male capable of taking all states in the behavioural space or is he dwelling in few of them only?

# 1 Introduction to *Drosophila* courtship

Innate courtship of the male fruit fly *Drosophila Melanogaster* consists of a series of behaviors which alternate in a complex pattern [2]. The courtship ritual of the male fly consists of a series of behaviours as orientation towards the female, wing extension and copulation. Figure 1 depicts courtship as a series of successive behaviours.

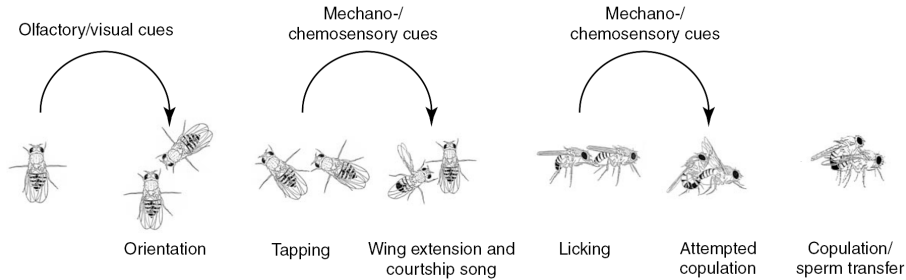


Figure 1: Courtship behaviours as presented by Billeter et al. [2]

However transitions between courtship behaviours seem probabilistic as the male fly can switch from any courtship behaviour to any other courtship behaviour [3, 5, 8]. Figure 2 presents an ethogram of courtship behaviour taken from Cobb et al. [5]: boxes denote to different courtship behaviours, while arrows between boxes indicate the probability of a switch through the arrow's thickness.

In the 1950s Margaret Bastock presented an idea to account for the problem of behavioural switches in innate fly courtship [9]. Her theory involves excitatory thresholds and varying excitation in the male fly. In the course of courtship male flies become increasingly sexually excited [9, 1, 18]. Courtship behaviours are assumed to be hierarchical in the level of excitation they require to be displayed [9]. Courtship is generated by one common network, with neuronal subsets sensitive to different excitatory frequencies [10]. The neural network determining courtship in the male fly consists of about 650 cells [10]. Through the use of genetic tools, it is possible to narrow down even smaller neuronal subsets which are responsible for specific courtship behaviours [11]. These neuronal subsets can be tested both for their necessity in generating a given behaviour (through neuronal deactivation) and their sufficiency in generating a behaviour (by artificial neuronal excitation). Thus *Drosophila* allows for a systematic study of behavioural choice.

## 2 Potential impact on animal replacement and healthcare

Research on fruit flies can replace clinical research on non-human vertebrates and is commonly used so already [12, 13, 14]. *Drosophila* courtship behaviour is not an obvious candidate for clinical research. However courtship behaviour of fruit flies has proven to be a useful measure of neurodegeneration and muscle deformation [12, 13, 14]. Physiological defects alter overall courtship levels.

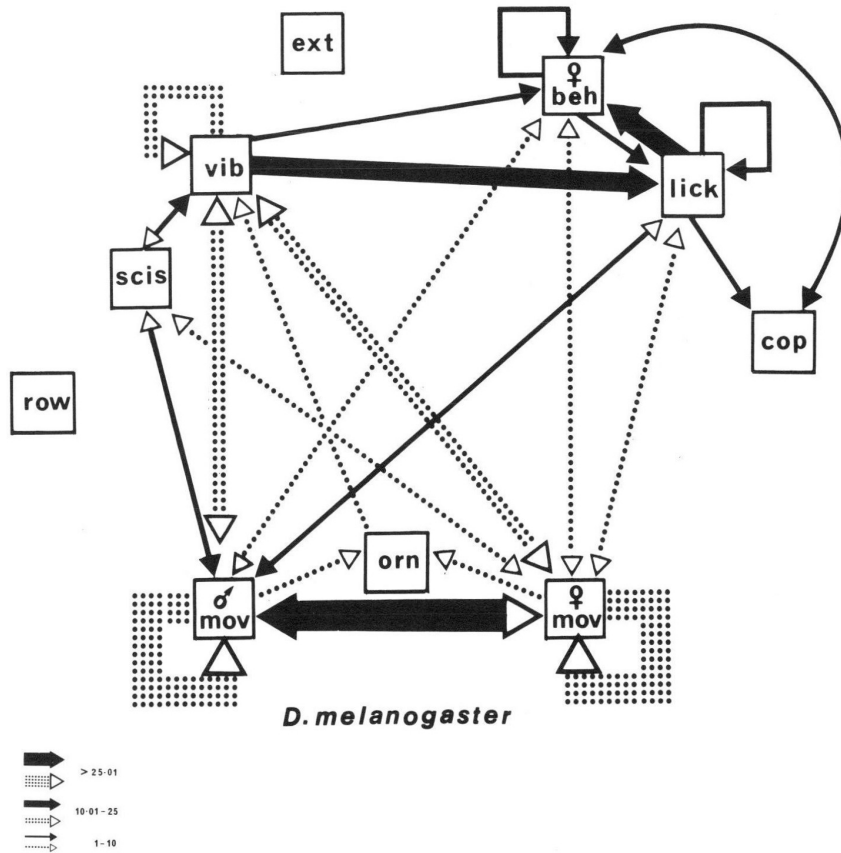


Figure 2: Ethogram of courtship behaviour for *Drosophila melanogaster*. Black arrows denote transitions significant at  $P \leq 0.01$ . The ethogram has been presented in Figure 5 of Cobb et al. [5].

Courtship is quantified mainly with summary measures as the percentage of time spent courting (CI). CI is easy to quantify and comprises courtship to one index. This allows for large scale comparisons. However simplifying courtship to one index omits differences in behavioural pattern. Courtship patterns are sensitive measures of the well-being of flies [9, 14]. Shaltiel-Karyo and colleagues found courtship to be reduced when they expressed a human gene associated with Parkinson’s disease (PD) in flies [14]. This illustrates the usefulness of *Drosophila* courtship for studying the genetic basis of human diseases.

Stochastic models of fly behaviour can illustrate subtle differences in behavioural patterns [15]. Thus stochastic models and their graphical implementation can act as tools to screen for and detect subtle differences in courtship patterns. We present here a first step towards a computational tool for illustrating courtship patterns.

There are different ways to model *Drosophila* courtship behaviour. During the workshop we have pursued both probabilistic and deterministic modelling approaches. Deterministic approaches require physiological parameters. However,

since there is little knowledge about relative strength of neuronal connections, we circumvent these types of models at the moment. Instead, we carefully chose our models to be informable with our behavioural data and to be in concordance with existing theories of courtship behaviour. Having models based on courtship behaviour, we can fit model parameters to given observations. We experimented with two deterministic models of neuronal activity. With them we started to test Margaret Bastocks hypothesis, which states that switches between courtship are due to hierarchical activity thresholds for successive courtship behaviours [9]. The two deterministic models we have studied have the advantage that they include a physiological mechanism. Each behaviour is seen as the result of neural activity, that triggers the behaviour when the activity or firing level is above a certain threshold.

Although this kind of model includes parameters which are difficult to estimate, parameter estimation is possible through established statistical tools as Approximate Bayesian Computation [21, 22].

### 3 Initial questions and objectives

At the beginning of the workshop we asked the following three questions:

1. Can we expand BBs courtship song model to courtship as a whole?

BB has developed a simple model of *Drosophila* courtship song (unpublished). Song consists of two qualitatively different modes: sine and pulse song. BBs model resorts to Margaret Bastock's hypothesis of hierarchical excitation thresholds to explain why a fly chooses to sing sine respectively pulse song [9]. In courtship song the experimental data basis is sufficient to develop a simple model of courtship song [16, 17, 19]. During the workshop we have found however that the data basis for courtship as a whole is not sufficient to model courtship as a function of realistic physiological processes. Song choice restricts analysis to wing movement, while courtship analysis has to account for movement of various body parts. The interaction between various body parts and underlying physiological mechanisms is yet subject to assumptions. We have started with testing whether the simple hypothesis of hierarchical excitation thresholds can account for switches between courtship behaviours.

2. How can we mine for possible models in large amounts of behaviour data?

We have used stochastic Markov processes to mine for behavioral patterns in normal and mutant flies. For stochastic models behaviour mining is a straightforward, well-known process. However, it is still a challenge to show that stochastic models are applicable and to minimize potential assumptions that come with model choices. For the Markov property to hold we require the process to be "memoryless", while this initially seems like a very strong assumption to make about the behaviour if it is indeed valid then the problem is mathematically far more approachable. To test the Markov property we needed to check whether the times spent in each state of courtship were distributed exponentially. Preliminary analysis indicated that the times did indeed seem to follow an exponential distribution. We have therefore shown that the underlying conditions for a Markov Model being applicable are not just assumed to be true, but indeed supported by our data.

3. What are advantages and disadvantages of these models?

This will be discussed below in the presentation of the respective models.

## 4 MATHEMATICAL MODELS

### 4.1 Probabilistic Model - Markov Process

In order to produce a model which was primarily data driven, we chose to implement a stochastic model. This approach allowed for a minimal assumption set and could have parameters which were found directly from the available data.

To begin constructing the stochastic model we first interrogate the existing data. In order to simplify the modelling we first checked whether the Markov property would hold for the system in question. The Markov property states that the next state of the system depends only on the current state and not on previous ones. This is a type of memoryless quality, however it does not necessarily imply that the male fly has no memory, just that the decisions made only depend on the current state. The Markov property requires that the dwell times in each state (that is, the amount of time spent in a state before changing state) must follow an exponential distribution. Since we already have access to a large amount of data this was checked by plotting the logarithm of the (1-CDF) function of each of the categories of dwell data. We can see that these plots appear to follow a straight line and we therefore conclude that the Markov property is a reasonable one to assume.

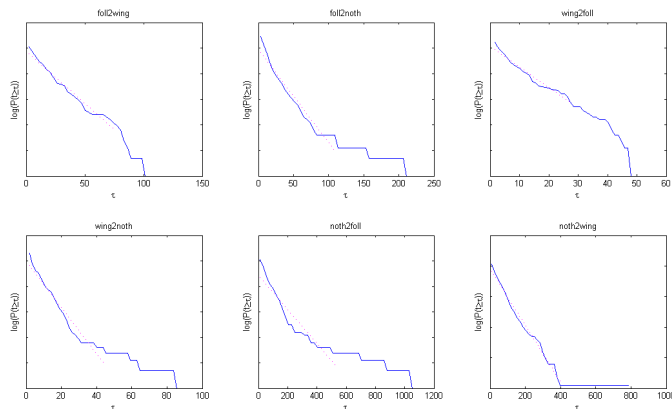


Figure 3: Logarithmic plots of the empirical 1-CDF for the observed data. The linearity of the plots near the Y-axis suggests that the Markov property is likely to be a reasonable feature to assume in the model.

We can now begin to define a continuous time Markov process to model the system. We choose a continuous time model since the actions of the fly occur in continuous time, even though the measurements taken are from video frames and are therefore discretised. We first define the state space and jump rates of the process. We use a random walk process on a graph with four nodes because the data available was scored into 4 categories: no courtship, following, wing extension and copulation.

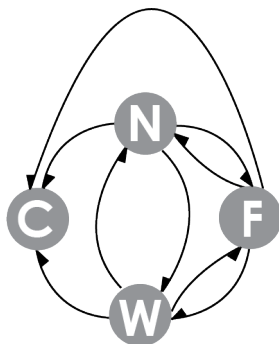


Figure 4: A schematic of the state space of the Markov process

#### 4.1.1 Model Definition

Let  $(\eta_t)_{t \geq 0}$  be an asymmetric random walk on the graph  $\Lambda_N$  of  $N$  nodes. The state of the process at time  $t$  which indicates which node the random walker occupies is denoted by  $\eta_t \in N, F, S, C$ . We denote the rate of jumping from state  $i$  to state  $j$  by  $\omega_{i,j}$ . We can therefore construct the jump matrix of the process according to the graph structure illustrated.

$$\mathbb{J} = \begin{pmatrix} -(\omega_{N,F} + \omega_{N,W} + \omega_{N,C}) & \omega_{F,N} & \omega_{W,N} & 0 \\ \omega_{N,F} & -(\omega_{F,N} + \omega_{F,W} + \omega_{F,C}) & \omega_{W,F} & 0 \\ \omega_{N,W} & \omega_{F,W} & -(\omega_{W,N} + \omega_{W,F} + \omega_{W,C}) & 0 \\ \omega_{N,C} & \omega_{F,C} & \omega_{W,C} & 0 \end{pmatrix}$$

From the jump matrix it is now possible to construct a master equation for the process to show how the probability density evolves across the state space in time.

$$\frac{d}{dt} \begin{pmatrix} \mathbb{P}(N) \\ \mathbb{P}(F) \\ \mathbb{P}(W) \\ \mathbb{P}(C) \end{pmatrix} = \mathbb{J} \times \begin{pmatrix} \mathbb{P}(N) \\ \mathbb{P}(F) \\ \mathbb{P}(W) \\ \mathbb{P}(C) \end{pmatrix}$$

Since this process has an absorbing state, i.e. once the process enters the copulation state it cannot leave, the stationary solution to the master equation is trivial and corresponds to all of the probability density being in the copulation state.

$$\frac{d}{dt} \begin{pmatrix} \mathbb{P}(N) \\ \mathbb{P}(F) \\ \mathbb{P}(W) \\ \mathbb{P}(C) \end{pmatrix} = \begin{pmatrix} 0 \\ 0 \\ 0 \\ 1 \end{pmatrix}$$

### 4.1.2 Simulations

In order to obtain a preliminary picture of whether the model outlined above can actually generate similar behaviour to that observed in actual courtship experiments we ran computer simulations of the process. This involved modelling a single object which could be in one of four states, corresponding to the states in the model above. Since we are assuming that the model is Markovian the wait times in any given state are distributed exponentially,

$$t \sim \lambda e^{-\lambda t}$$

with  $\frac{1}{\lambda}$  being the mean wait time in the state. It is then possible to draw a (pseudo)random time from this distribution using the inverse CDF method such that

$$t = -\frac{\ln(x)}{\lambda},$$

where  $x \in (0, 1)$  is a pseudorandom number drawn from a uniform distribution on the unit interval.

This is all that is required to simulate the switching between states that we wish to model. We then ran this simulation using mean wait time which were calculated from the experimental data which we had. This could then be used to generate an ethogram in a similar fashion to the ones shown in the data.

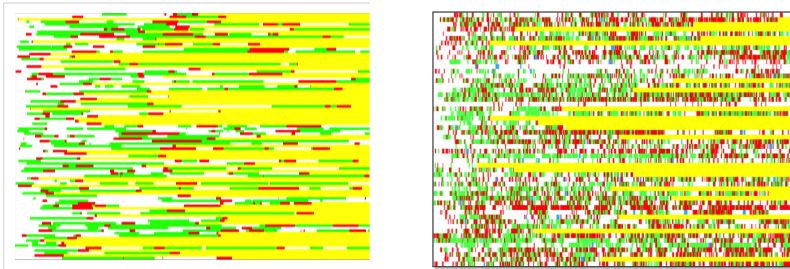


Figure 5: Left: An ethogram of behaviours exhibited over time generated from the simple random walk model. Right: An example of a real ethogram produced from analysing courtship videos.

The ethograms generated appear to follow similar patterns to the real data obtained from courtship videos. In order to quantify the closeness of the generated data to that obtained from experiment we need to define a metric. This will allow us to determine the optimum parameters to generate data which is closest to that observed. This will hopefully also show the validity of the assumptions in the model if the fitted rates are close to those which are calculated from the data.

This model can be expanded by applying it to other graph structures for the behavioural states. This could allow for the inclusion of a richer set of states or potentially applications to other behaviours than courtship.

## 4.2 Neuronal Models

When modelling the courtship patterns of *Drosophila melanogaster*, it has been observed that certain neurons fire during the differing stages of courtship. We decided to focus upon a simple model of four neuron clusters, namely: Processing unit ( $P$ ), which corresponds to no behaviour; Following cluster ( $F$ ), which in fact comprises several neuron types activated while following behaviour is displayed; Wing vibration cluster ( $W$ ), more precisely defined as mesothoracic cluster; and finally Copulation cluster ( $C$ ), located in the abdomen. As a simple starting point, we are going to consider these four neuronal clusters interconnected with differently weighted excitatory and inhibitory connections between them. For simplicity, we assume that the neurons in one cluster fire at the same time, so that we can model each cluster as a single neuron. There are biological reasons to consider each cluster modelled as one neuron. Each of the behaviours can be linked to a group of neurons which share a specific feature, for example an active gene sequence. When these neurons are activated *at the same time*, the behaviour is displayed. Hence we can justify model a set of neurons with one neuron both with those neurons all sharing one biological feature (active gene sequence) and with observing behaviour when all neurons in that given set are activated at the same time.

In the following, two different models are introduced to describe the interconnections among these neuronal clusters: a simple difference equations system and a Fitzhugh-Nagumo one. If the models outputs fit well the observed behavioural data, they will potentially have a great value in identifying impaired neural connections in neurodegenerative cases.

### 4.2.1 Pasemann-like Model

In the '90s, Pasemann proposed a simple model to describe interactions between neurons [23, 24]. Here the dynamics of neuronal interactions are described by discrete-time difference equations. To every “unit” (neuron)  $i$  corresponds one equation describing its *activation*  $a_i$  which is defined by

$$a_i = \sum_j w_{ij} o_j + \theta_i$$

where  $w_{ij}$  is the *weight* assigned to the connection between the units  $i$  and  $j$  ( $i \neq j$ ),  $\theta_i = \bar{\theta}_i + I_i$  ( $I_i$  total “external” input to unit  $i$ ,  $\bar{\theta}_i$  fixed bias) and  $o_j$  represents the *output* coming from unit  $j$ . The output function is taken to be

$$o_j = \sigma(a_j) = \frac{1}{1 + e^{-a_j}} .$$

Note that  $\sigma$ -functions are a standard way to describe a “smooth” switch.

The model presently developed consists of the four units (neural clusters) described above, which interact as described in Figure 6. It is stressed that few is known about these connections. Therefore, on one hand it is difficult to realistically estimate the parameters, but on the other the model has the potential of giving great insight into the understanding of the system.

Being no specific data to inform the weight choice, the numbers associated to the various connections shown in Figure 6 are simply the times (over four experiments) in which the corresponding behavioural transition is observed;

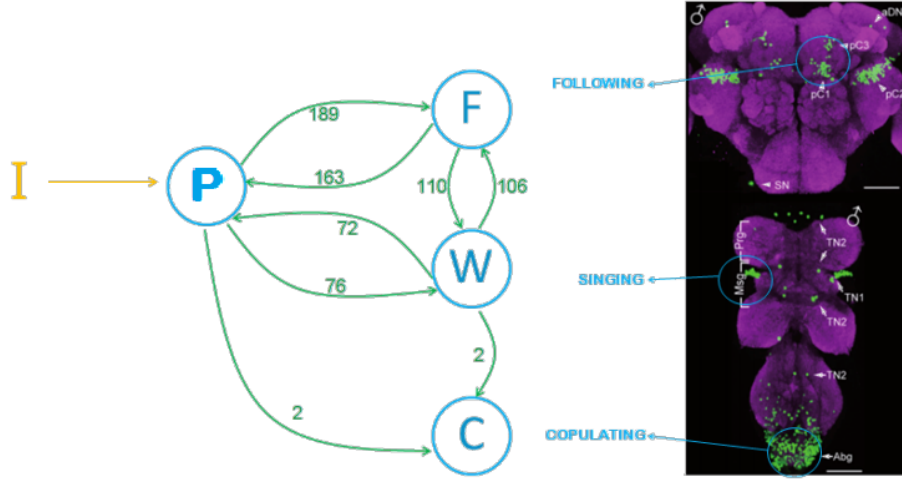


Figure 6: Schematic view of the model, compared with a photo of the actual clusters in the *Drosophila*'s brain and ventral nerve cord. The numbers on the edges are the number of times the corresponding behavioural switch is observed during four experiments.

then the considered weights will be these numbers divided by 4. In this way, it is implicitly assumed that each behavioural switch is proportional to the weight of the corresponding connection. However, this assumption is just taken as a starting point to associate numbers to the weights, and further work will be done to have better estimates of the model parameters.

In writing the equations describing the activity of each cluster, it is assumed that the clusters  $F$  and  $W$  reciprocally reduce the output coming from the processing unit  $P$ , and this output is also reduced by the activity of  $C$ . More precisely, being  $F_n$  the activation of the cluster  $F$  at time  $n$ , the value of  $F_{n+1}$  is given by  $w_{PF}\sigma(P_n) \cdot \sigma(F_n - W_n - C_n) + w_{WF}\sigma(W_n)$ , where the second term is due to the connection from  $W$  to  $F$  shown in the diagram, and the former term takes into account the connection from  $P$  to  $F$  "reduced" by the activity of the clusters  $W$  and  $C$ . This approach will hopefully take into account a sort of "hierarchy" among the neural clusters: it is observed that for example copulation is "stronger" than following and wing extension, so we hope to see a kind of ordered sequence in the behaviours emerging from this neural activity.

Applying similar reasoning for all the four units, the equations describing the network are

$$\begin{aligned}
 P_{n+1} &= I_n + w_{FP}\sigma(F_n) + w_{WP}\sigma(W_n) \\
 F_{n+1} &= [w_{PF}\sigma(F_n - W_n - C_n)] \cdot \sigma(P_n) + w_{WF}\sigma(W_n) \\
 W_{n+1} &= [w_{PW}\sigma(-F_n + W_n - C_n)] \cdot \sigma(P_n) + w_{FW}\sigma(F_n) \\
 C_{n+1} &= [w_{PC}\sigma(F_n + W_n)] \cdot \sigma(P_n) + w_{WC}\sigma(W_n)
 \end{aligned}$$

where  $I_n$  denotes the external stimulus at time  $n$ . Note that  $I_n$  here depends on the female response at time  $n$ , and in a first instance it is considered to be random.

A first numerical simulation of the model (performed in MatLab) can be

appreciated in Figure 7 where the neuronal activity of the different clusters is plotted for about 60 time steps.

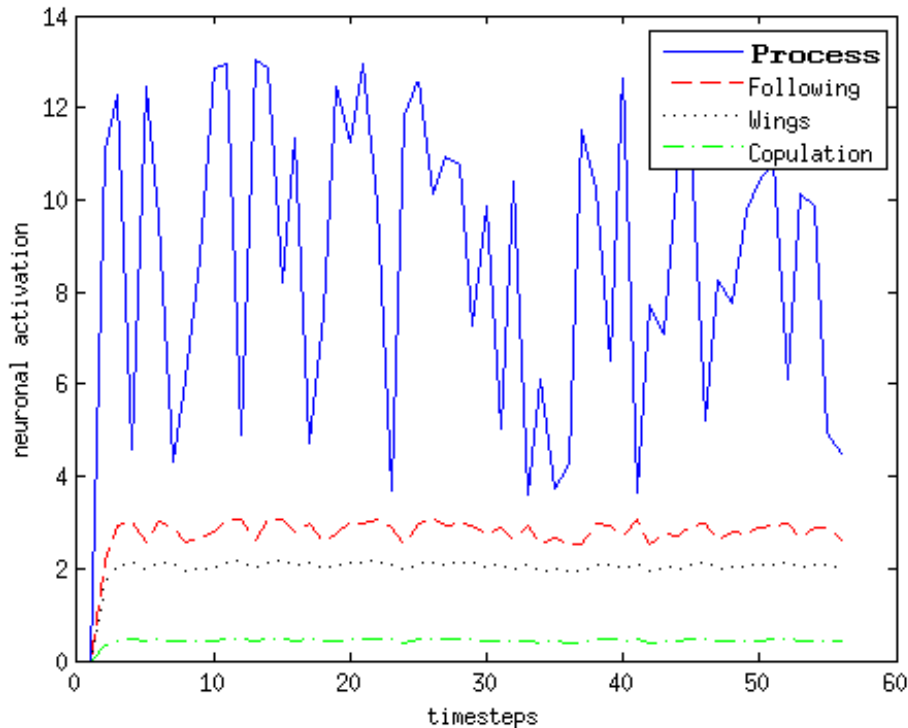


Figure 7: Simulation of neural activity of the four neural clusters.

The simulation shows that in this case the system very quickly reaches a kind of “equilibrium”, having the different cluster activities oscillating around a fixed value.

To convert these results into behavioural output (which would then be comparable with real data), it then assumed that a certain behaviour is displayed by the fly when the activation of the corresponding neural unit is above a certain threshold. Therefore, Figure 8 shows the “translation” of the dynamics shown in Figure 7: here we have a pattern of the same form of the available behavioural data.

Although it is still early to decide whether this output is “good” or not, this preliminary result shows that this neural approach might be a good way to study the model. In fact, it produces an output which is comparable with the experiments, and the general shape of the network is based on widely accepted biological knowledge.

The main aspect of this model can be largely improved is the parameter estimation. The neuronal activation presently considered does not correspond to a precisely defined physical quantity, and it seems difficult to practically implement an experiment measuring the weight of a connections between clusters. However, the data contained in the ethograms can be used to estimate the weights and the thresholds in the normal case. Then, if the model results fit the biological observations, this system could be used to speculate about the most

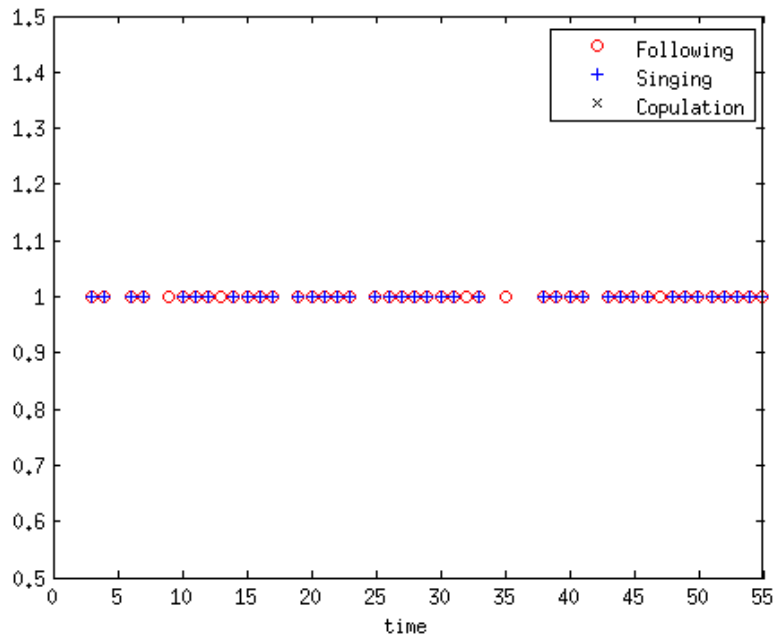


Figure 8: Behavioural pattern emerging from the previous simulation of neural activation.

relevant connections between neurons. This would have a big impact in studying the underlying mechanisms of impaired neural activity as the one observed in Parkinson's disease.

### 4.2.2 Other Mathematical Models of Neurons and Simple Networks

In 1943, McCulloch and Pitts [25] devised a simple mathematical model of a neuron which subsequently led to the development of the field of Artificial Neural Networks (ANNs), see [26] for an introduction to ANNs. The artificial neuron is made up of four basic components: an input vector, say  $x_j$ , a set of synaptic weights, say  $w_{ij}$ , a summing junction with an activation (transfer) function, say  $\phi$ , and an output, usually denoted by  $y_i$ . The model describes a neuron acting like a binary processing unit, where

$$y_i = \phi \left( \sum_j w_{ij} x_j \right)$$

and  $\phi$  is usually a sigmoid function. Unfortunately, this simple binary model is not suitable for real biological neurons. In 1952, Alan Lloyd Hodgkin and Andrew Huxley were modelling the ionic mechanisms underlying the initiation and propagation of action potentials in the giant squid axon [27]. By treating each component of the excitable cell as an electrical element, and applying the conservation of electric charge on a piece of membrane, they were able to derive a set of Ordinary Differential Equations (ODEs) for membrane current density, see [26] for more information. The Hodgkin-Huxley (HH) ODEs have served as a classic reference in brain science and neurophysiology for several decades, unfortunately, these equations did not have a sound circuit theoretic foundation but were derived using empirical methods. In [28, 29], Chua et al. show that sodium and potassium ion-channel memristors are the key to generating the action potential in the HH ODEs, and that they are the key to resolving several unresolved anomalies associated with these ODEs.

Many mathematical neuronal models have been developed since the publication of the HH paper, simplified models directly relevant to this project are highlighted here. In 1961 and 1962, Fitzhugh [30] and Nagumo [31], respectively, derived a set of ODEs (essentially a reduction of the HH ODEs) to model the activation and deactivation dynamics of a spiking neuron. The describing Fitzhugh-Nagumo (FN) ODEs are:

$$\frac{dv}{dt} = c \left( v - \frac{v^3}{3} + w + I \right), \quad \frac{dw}{dt} = \frac{1}{c} (a - v - bw), \quad (1)$$

where  $v$  is a fast variable (in biological terms - the action potential),  $w$  represents a slow variable (biologically - the sodium gating variable), and  $I$  is the magnitude of stimulus current. The parameters  $a$ ,  $b$  and  $c$  dictate the threshold, oscillatory frequency and the location of the critical points for  $v$  and  $w$ . A neuron will begin to oscillate when the input current  $I$  is above a critical threshold  $I_T$ , say.

A spiking-bursting ODE model of a neuron was introduced by Hindmarsh and Rose [32] in 1984, the three-dimensional system of ODEs has the form

$$\frac{dx}{dt} = y + f(x) - z + I, \quad \frac{dy}{dt} = g(x) - y, \quad \frac{dz}{dt} = r [s(x - x_R) - z], \quad (2)$$

where  $f(x) = -ax^3 + bx^2$ , and  $g(x) = c - dx^2$ ,  $x$  is the membrane potential,  $y$  represents the transport of sodium and potassium through fast ion channels, and  $z$  is the transport of other ions through slow channels,  $x, y, z$  are dimensionless

quantities here. This simple model allows a good qualitative description of many different patterns of experimentally observed action potentials.

Arguably, the best simplified model to demonstrate most of the neuronal dynamics displayed experimentally is that devised by Izhikevich [33] in 2003, although the model is biophysically meaningless. The ODEs are given by

$$\frac{dv_1}{dt} = 0.04v_1^2 + 5v_1 + 140 - v_2 + I, \quad \frac{dv_2}{dt} = \alpha(\beta v_1 - v_2), \quad (3)$$

with the auxiliary after-spike resetting

$$\text{if } v_1 \geq 30\text{mV, then } \begin{cases} v_1 \leftarrow c \\ v_2 \leftarrow v_2 + d. \end{cases} \quad (4)$$

The variable  $v_1$  represents the membrane potential,  $v_2$  is a membrane recovery variable,  $\alpha$  describes the time scale of the recovery variable  $v_2$ ,  $\beta$  determines the resting potential of the neuron, and other parameters in (3) were chosen so that outputs aligned with human neurons. When the spike reaches 30 mV, the membrane voltage and the recovery variable are reset according to (4). In 2004, Izhikevich [34] compared the biological plausibility and computational efficiency of the following mathematical models: the HH model [27], the FN model [30, 31], the HR model [32], the Morris-Lecar (ML) model [35] and the spiking model of Izhikevich [33]. The HH and ML models are biophysically relevant, however, highly connected networks of these modelled neurons are computationally inefficient. The Izhikevich model is the computationally most efficient model capable of computing hundreds of thousands of interconnected neurons, however, they are biophysically meaningless.

We have carried out preliminary investigations for the simplest and most meaningful ODE model listed above, namely the FN ODE model (1). *Drosophila melanogaster* has different classes of neurons with different properties. We decided to reduce our study of neuron features on neuronal thresholds, as neuronal excitation is known to drive switches between courtship behaviours [17]. Different neural thresholds of each courtship behaviour are one possibility to explain this observation. By changing the parameter  $c$  in the ODEs (1) we can alter the threshold of the neuron. For example, when  $c = 3$  the threshold is approximately 0.4mV, and the amplitude of oscillation is approximately 2 units (see Figure 9), and when  $c = 1$ , the threshold is approximately 0.8mV, and the amplitude is approximately 0.5 units. Figure 9(a) shows that the threshold of the neuron is not reached and hence it does not fire, when the input exceeds  $I \approx 0.4\text{mV}$ , the neuron starts to fire with a frequency of about 0.073kHz, and when  $I \approx 0.6$ , the frequency has risen to approximately 0.098kHz. Figure 10 shows how the neuron firing frequency changes with respect to neuron input magnitude. Note that, with the FN model, as the input increases beyond  $I \approx 1\text{mV}$ , the frequency starts to drop again and eventually the solution jumps to the other stable critical point and the neuron ceases firing once more. Physically, once the threshold is attained the neuron will continue to fire at an increasing frequency up to some physical limit. Thus, using the FN ODE model it is possible to have neurons with different thresholds and having different firing frequencies. Next we want to model how the neurons, and eventually the neuron clusters, are connected. As a simple starting point we will consider linearly coupled FN models as depicted

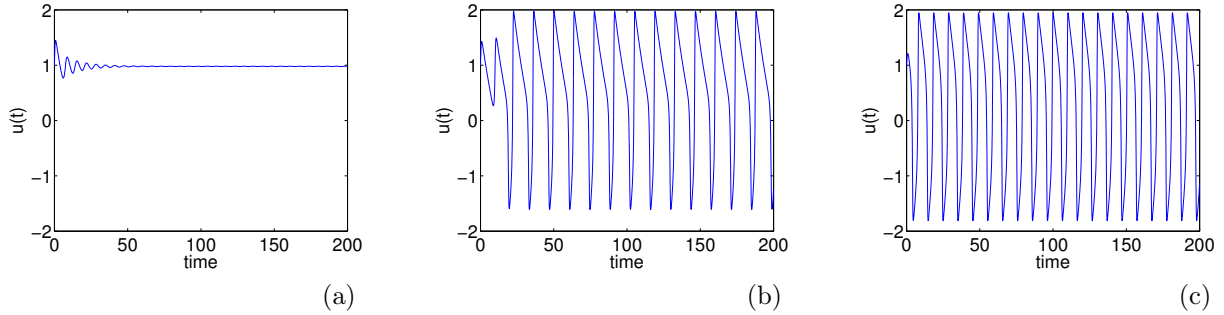


Figure 9: (a) Consider system (1), when the input is  $I = 0.38\text{mV}$ , the neuron does not fire; (b) when the input is  $I = 0.4\text{mV}$ , threshold is achieved and the neuron starts spiking; (c) as the input increases to  $I = 0.5\text{mV}$ , the frequency of firing increases.

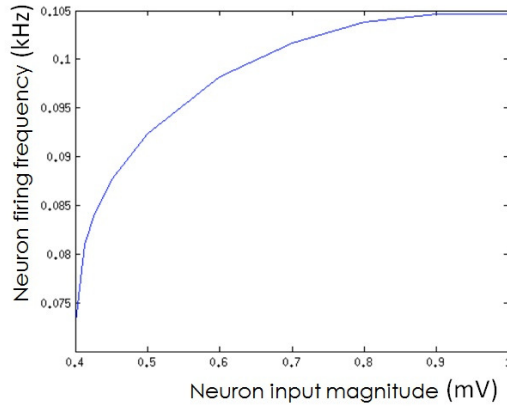


Figure 10: Graph of neuron firing frequency with respect to neuron input magnitude.

in system 5

$$\begin{aligned} \frac{dv_1}{dt} &= c \left( v_1 - \frac{v_1^3}{3} + w_1 + I + k \left( \frac{dv_2}{dt} - \frac{dv_1}{dt} \right) \right), & \frac{dw_1}{dt} &= \frac{1}{c} (a - v_1 - bw_1), \\ \frac{dv_2}{dt} &= c \left( v_2 - \frac{v_2^3}{3} + w_2 + I + k \left( \frac{dv_2}{dt} - \frac{dv_1}{dt} \right) \right), & \frac{dw_2}{dt} &= \frac{1}{c} (a - v_2 - bw_2), \end{aligned} \quad (5)$$

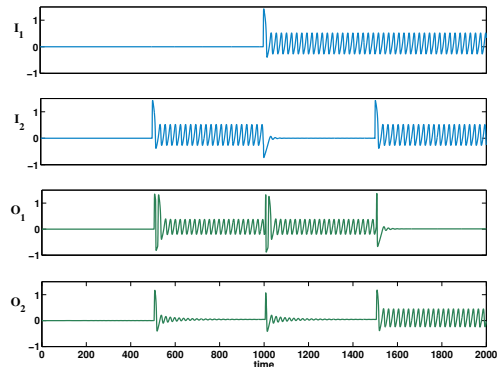
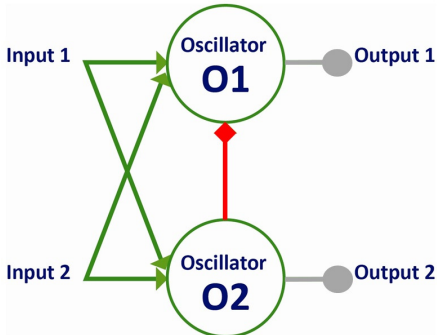
where  $k$  is a coupling coefficient.

A far more realistic coupling between neurons is provided by transfer functions of the form

$$\sigma(x) = \frac{1}{1 + e^{m(\tau-x)}}, \quad (6)$$

where  $\tau$  determines a threshold and  $m$  denotes the steepness of the curve.

In 2009, Borresen and Lynch [36] coupled HH ODEs together using a transfer function of the form (6) and demonstrated logical AND and OR operations



(a)

(b)

Figure 11: (a) Schematic of a binary oscillator half adder comprising two inputs  $I_1$  and  $I_2$ , two oscillators  $O_1$  and  $O_2$  and a set of excitatory synaptic connections with weights  $w_1, w_2$ , and an inhibitory connection with weight  $x_1$ . The sum oscillator  $O_1$  will oscillate if either  $I_1$  or  $I_2$  are active. The carry oscillator  $O_2$  will oscillate if both  $I_1$  and  $I_2$  are active. The inhibitory connection  $x_1$ , from  $O_2$  to  $O_1$  suppresses oscillator  $O_1$  if  $O_2$  is active. (b) Time series showing that the half-adder is functioning correctly when the oscillations are simulated using Fitzhugh-Nagumo systems. Oscillations are equivalent to a binary one in these simulations and no oscillation is zero.

of HH neurons. Three years later, these ideas were galvanized and an international patent was published [37]. The patent illustrates how it is possible to construct binary logic gates from coupled threshold oscillators connected using both excitatory and inhibitory connections. Figure 11 displays the schematics of the binary oscillator half-adder along with the corresponding time series of input/output. The simulations were run based on FN oscillators [38].

In future work we will also need to model using Delay Differential Equations (DDEs) since delays are inherently present in neuronal networks.

## 5 Workshop outcome and future work

We have followed up our work in Cambridge during a meeting in Oxford. We met for five days between November 19th and November 23rd 2014. During this meeting we presented our work to mathematicians and fly biologists in Oxford. We have received helpful feedback on our work. In specific we were able to improve our markovian courtship simulations and inform our neuronal models with up-to-date physiological knowledge of courtship neurons.

During the November meeting we were able to link our markovian random-walk model with our Paseman-like neuronal model. While the random-walk model allows for rapid simulations, the Paseman-like model might allow insights of mechanistic nature. For example we can address the question "What distinguishes a neuronal network giving rise to normal and impaired courtship?". For studying this question we have recently contacted biologists specialised in

Parkinson research in *Drosophila* who published courtship data of healthy flies as well as flies expressing a human Parkinson gene [14]. We would like to collaborate with them as we believe a collaboration increases the value of our modelling work and strengthens their argument of fly courtship as a valuable assay to quantify neuronal impairments.

The results we obtained during the NC3R's POEMs workshop show that male courtship is no fixed behavioural chain, started once unwinding all components, but instead switches between courtship require external excitation, which can be modelled as a random process.

#### ACKNOWLEDGEMENTS

The authors acknowledge support from the NC3Rs and the POEMs network who have funded both the Mathematics Study Group in Cambridge and our follow-up meeting in Oxford.

## References

- [1] Arthur, B.J. et al. (2013) *Multi-channel acoustic recording and automated analysis of Drosophila courtship songs*. BMC Biol. 11, 1–11
- [2] Billeter, J.-C. et al. (2006) *Control of male sexual behavior in Drosophila by the sex determination pathway*. Curr. Biol. 16, 766–776
- [3] Bastock, M. and Manning, A. (1955) The Courtship of *Drosophila melanogaster*. Behaviour 8, 85–111
- [4] Bastock, M. (1956) *A Gene Mutation Which Changes a Behavior Pattern*. Evolution (N. Y). 10, 421–439
- [5] Cobb, M. et al. (1989) Courtship in *Drosophila sechellia*: Its structure, functional aspects, and relationship to those of other members of the *Drosophila melanogaster* species subgroup. J. Insect Behav. 2, 63–89
- [6] Coen, P. et al. (2014) Dynamic sensory cues shape song structure in *Drosophila*. Nature DOI: 10.1038/nature13131
- [7] Kohatsu, S. et al. (2011) *Female contact activates male-specific interneurons that trigger stereotypic courtship behavior in Drosophila*. Neuron 69, 498–508
- [8] Markow, T.A. and Hanson, S.J. (1981) Multivariate analysis of *Drosophila* courtship. Proc. Natl. Acad. Sci. U. S. A. 78, 430–434
- [9] Bastock, M. (1956) A Gene Mutation Which Changes a Behavior Pattern. Evolution (N. Y). 10, 421–439
- [10] Rideout, E.J. et al. (2010) Control of sexual differentiation and behavior by the doublesex gene in *Drosophila melanogaster*. Nat. Neurosci. 13, 458–466
- [11] Pavlou, H.J. (2014) , Intersecting doublesex neurons underlying sexual behaviours in *Drosophila melanogaster*. University of Oxford, U.K.

- [12] Chakravorty, S. et al. (2014) Mutations of the *Drosophila* myosin regulatory light chain affect courtship song and reduce reproductive success. *PLoS One* 9, e90077
- [13] McBride, S.M.J. et al. (2005) Pharmacological rescue of synaptic plasticity, courtship behavior, and mushroom body defects in a *Drosophila* model of fragile X syndrome. *Neuron* 45, 753–764
- [14] Shaltiel-Karyo, R. et al. (2012) A novel, sensitive assay for behavioral defects in Parkinson’s disease model *Drosophila*. *Parkinsons. Dis.* 2012, 1–6
- [15] Berman, G.J. et al. (2014) Mapping the stereotyped behaviour of freely moving fruit flies. *J. R. Soc. Interface*, 11, 20140672
- [16] Clyne, J.D. and Miesenböck, G. (2008) Sex-specific control and tuning of the pattern generator for courtship song in *Drosophila*. *Cell* 133, 354–363
- [17] Pan, Y. et al. (2012) Joint control of *Drosophila* male courtship behavior by motion cues and activation of male-specific P1 neurons. *Proc. Natl. Acad. Sci. U. S. A.* 109, 10065–10070
- [18] Pan, Y. et al. (2011) *Turning males on: activation of male courtship behavior in Drosophila melanogaster*. *PLoS One* 6, e21144
- [19] Shirangi, T.R. et al. (2013) Motor control of *Drosophila* courtship song. *Cell Rep.* 5, 678–686
- [20] Lee, G. et al. (2000) *Spatial, temporal, and sexually dimorphic expression patterns of the fruitless gene in the Drosophila central nervous system*. *J. Neurobiol.* 43, 404–426
- [21] Liepe, J. et al. (2014) *A framework for parameter estimation and model selection from experimental data in systems biology using approximate Bayesian computation*. *Nat. Protoc.* 9, 439–456
- [22] Toni, T. et al. (2009) *Approximate Bayesian computation scheme for parameter inference and model selection in dynamical systems*. *J. R. Soc. Interface* 6, 187–202
- [23] Pasemann, F. (1993) Discrete Dynamics of Two Neuron Networks. *Open Systems & Information Dynamics* 2(1) 49–66
- [24] Pasemann, F. (1995) Neuromodules: A dynamical systems approach to brain modelling. Herrmann, H., Pöppel, E. & Wolf, D. (eds.) *Supercomputing in Brain Research - From Tomography to Neural Networks* 331–347
- [25] W. McCulloch and W. Pitts, A logical calculus of the ideas immanent in nervous activity, *Bulletin of Mathematical Biophysics*, **5** (1943), 115–133.
- [26] S. Lynch, *Dynamical Systems with Applications using MATLAB<sup>®</sup>* 2nd Edition, Springer International Publishing, 2014.
- [27] A.L. Hodgkin and A.F. Huxley, "A qualitative description of membrane current and its application to conduction and excitation in nerve," *J. Physiol.* **117**, 500–544, 1952. Reproduced in *Bull. Math. Biol.*, **52** (1990) 25–71.

- [28] L. Chua, V. Sbitnev and H. Kim, Hodgkin-Huxley axon is made of memristors, *Int. J. Bifurcation Chaos* **22** (2012) 1230011.
- [29] L. Chua, V. Sbitnev and H. Kim, Neurons are poised near the edge of chaos, *Int. J. Bifurcation Chaos* **22** (2012) 1250098.
- [30] R. Fitzhugh, "Impulses and physiological states in theoretical models of nerve membranes," *Biophys.*, **1182** (1961) 445–466.
- [31] J. Nagumo, S. Arimoto and S. Yoshizawa, "An active pulse transmission line simulating 1214-nerve axons," *Proc. IRL* **50** (1970) 2061–2070.
- [32] J.L. Hindmarsh and R.M. Rose, A model of neuronal bursting using three coupled first order differential equations. *Proc. R. Soc. London, Ser. B* **221** (1984) 87102.
- [33] E.M. Izhikevich, Simple Model of Spiking Neurons, *IEEE Transactions on Neural Networks* **14**(6) (2003) 1569–1572.
- [34] E.M. Izhikevich, Which model to use for cortical spiking neurons?, *IEEE Transactions on Neural Networks* **15**(5) (2004) 1063–1070.
- [35] C. Morris and H. Lecar, Voltage oscillations in the barnacle giant muscle fibre, *Biophys. J.* **35** (1981) 193–213.
- [36] J. Borresen and S. Lynch, Neuronal computers, *Nonlinear Anal. Theory, Meth. & Appl.*, **71** (2009) 2372–2376.
- [37] S. Lynch and J. Borresen, Binary Half Adder using Oscillators, *International Publication Number, WO 2012/001372 A1* (2012) 1–57.
- [38] J. Borresen and S. Lynch S, Oscillatory Threshold Logic. *PLoS ONE* 7(11): e48498. doi:10.1371/journal.pone.0048498 (2012).